Automatic MRI Database Exploration and Applications

Alexandre Guimond, Gérard Subsol, Jean-Philippe Thirion

AUTOMATIC MRI DATABASE EXPLORATION AND APPLICATIONS

ALEXANDRE GUIMOND*, GÉRARD SUBSOL
and JEAN-PHILIPPE THIRION

Institut National de Recherche en Informatique et en Automatique
2004, Route des Lucioles B.P. 93, 06902 Sophia-Antipolis Cedex, France
E-mail: {*Alexandre.Guimond, Gerard.Subsol, Jean-Philippe.Thirion*}*@sophia.inria.fr*

The design of representative models of the human body is of great interest to medical doctors. Qualitative information about the characteristics of the brain is widely available, but due to the volume of information that needs to be analyzed and the complexity of its structure, rarely is there quantification according to a standard model. To address this problem, we propose in this paper an automatic method to retrieve corresponding structures from a database of medical images. This procedure being local and fast, will permit navigation through large databases in a practical amount of time. We present as examples of applications the building of an average volume of interest and preliminary results of classification according to morphology.

Keywords: Image database, exploration, volume of interest (VOI), average patient, medical atlas, classification, registration, magnetic resonance imaging (MRI).

1. INTRODUCTION

Neurological disorders like schizophrenia or Alzheimer's disease have for long been the subject of serious studies. It is believed that such conditions could be coupled with abnormal configurations of different brain structures, but strong quantitative evidence has still to be reported. Although anatomical brain atlases[1–4] provide information to analyze and compare brain structures, their characteristics, such as precise shape and variance among healthy subjects, are not yet clearly defined. Moreover, paper representations are not sufficient to answer today's problems in this field;[5,6] such atlases are two-dimensional, static and based on one or few studies. Computer guided diagnosis, multimedia medical teaching or surgical simulation robotics require more adaptable and complete sources of information.

Over recent years, the use of magnetic resonance imaging (MRI) has produced huge medical brain image databases. Study of these data could provide the information needed to build numerical atlases with quantification of brain structure characteristics. This article addresses the problem of exploring such databases to retrieve information about a specific part of the brain (see Fig. 1). The idea is to provide tools for practitioners to define a volume of interest (VOI) within a patient's MRI and extract corresponding VOIs from the database. These VOIs can be viewed as either control subjects or representative elements of different classes of pathology. In the first case, contrast images would facilitate the identification of

*The author is visiting from the Département d'Informatique et de Recherche Opérationnelle de l'Université de Montréal (Canada).

International Journal of Pattern Recognition and Artificial Intelligence Vol. 11 No. 8 (1997) 1345–1365

2.1. Previous Work

Many matching methods have been put forward to identify differences between brain images (see Ref. 7 for a comprehensive review). They can be divided in two main categories: feature-based[8–11] and intensity-based,[12–15] the trade-off being between the size of the data to register and the complexity of the registration procedure.

The class of transformation T used is also important. Various approaches exist. To name a few, registration methods have been developed using linear,[16–18] piecewise linear,[19] quadratic[20] and free-form,[12,13] classes (see Fig. 2 for a rough classification).

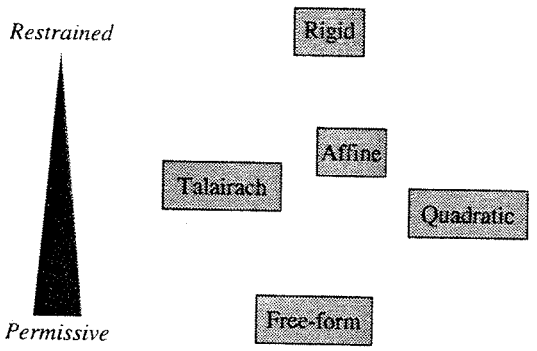

Fig. 2. Classification of different transformation classes.

A very common approach is to use the Talairach reference space, also known as the three-dimensional proportional grid system.[1] This system uses the bicommissural line and some other anatomical landmarks to partition the brain into twelve subspaces and is an attempt to model the nonlinear differences between data sets (see Fig. 3).

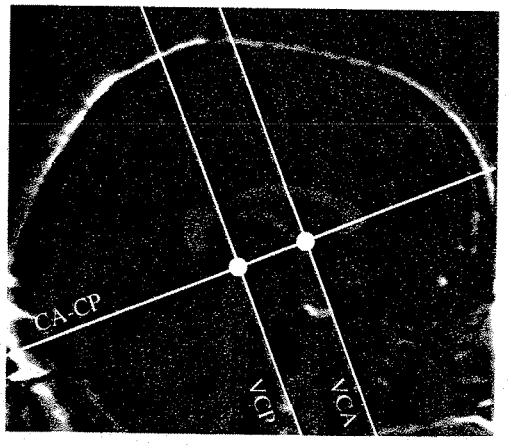

Fig. 3. Sagittal view of the Talairach divisions.

phological variations. The subject on the left has two gyri and the one on the right only one. These are non-trivial differences since they require the location of absent features.

Morphometrical: These are variations due to the different properties of *existing* features. For example, the length of a gyrus or the volume of the ventricles (Fig. 4 presents two patients with different ventricle volumes). For the purpose of this article, morphometrical variations will be divided in three categories:

Global: Brain scale morphometrical variations.

Regional: VOI scale morphometrical variations.

Local: Voxel scale morphometrical variations.

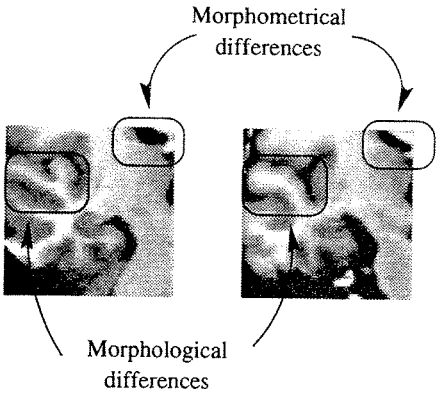

Fig. 4. Morphometrical and morphological differences.

3.2. Irrelevant Variations

As previously mentioned, our interest lies in the study of particular brain structures. In that respect, it is generally agreed that for the vast majority of subjects, global morphometrical differences, such as the width or the length of the whole brain, are not really significant. Furthermore, this idea can hold for differences between sufficiently large VOIs. Our registration method will reflect those assumptions by correcting for affine differences at global and regional scales. This class of transformation will correct translation, rotation, scale and skew differences between VOIs.

Choosing this transformation class has some advantages over the Talairach alternative. The proportional grid system is a reference space that is frequently used by medical doctors, which is an important asset since they are the end-users. But it shows poor accuracy when matching structures away from the anterior and posterior commissures and limits the extraction procedure to the brain.

It is worth noting that correcting for affine differences between VOIs is in agreement with the Talairach philosophy of not considering structures away from the

Global morphometrical corrections. The global correction procedure consists in *estimating* an affine transformation to map the database entry dimensions to the ones of the reference image. This step is necessary to extract grossly corresponding VOIs needed for regional comparisons in the second step. To reduce computation, the matching is done on sub-sampled images, a justifiable approach since we are only looking for a gross correspondence.

Before registration, we apply to each of the two images the following transformations:

1. A transformation A to a standard axis view and voxel size. In our case these are coronal views and $1 \times 1 \times 1$ mm^3 per voxel. This transformation ensures that images coming from different sources are comparable.
2. A resampling using the scale parameter S_g to the desired resolution for global registration. In practice, this is a useful parameter that influences the precision of the transformation obtained and the computation time.

After matching, we obtain the global affine transformation G.

Regional morphometrical corrections. This procedure is similar to the previous one. Two steps differ. The first modification concerns the database entry for which we substitute the change of referential by the global correction matrix G. As a second difference, the scaling factor for global registration S_g is replaced by its local equivalent S_l and a transformation E accounting for the VOI extraction. This last transformation is a cropping at identical locations for both images. In our work, it is implemented using a translation, to make it representable using matrices and a size specification. This matching provides the regional affine transformation R.

Local morphometrical corrections. Evaluation of local differences is done using the same procedure as before, with a correction matrix R updated with regional information, and a matching allowing a transformation class T of the free-form type.

Images after the regional correction are called *corresponding volumes of interest.* They differ only by morphological and local morphometrical variations. Hence, when considering structures of the same morphology, images can be used to obtain information concerning morphometrical dissimilarities such as size differences.

Morphological variations can be obtained by applying the third step that corrects for local morphometrical differences. From this, the detection of particular features could be obtained.

An interesting aspect of our work is the combination of those transformations by way of 4×4 matrices in homogeneous coordinates, and optionally a displacement field derived from local variations, which ends up with a single transformation and therefore a single resampling of the raw images.

It is also possible to completely eliminate the first part of the procedure since, for a given reference image, these transformations do not depend on the VOI definition. They can be precomputed to save time. Moreover, when the reference image changes, instead of recomputing the whole set of global transformations, it is sufficient to combine them with the transformation that brings the old reference image onto the new one (see Fig. 6).

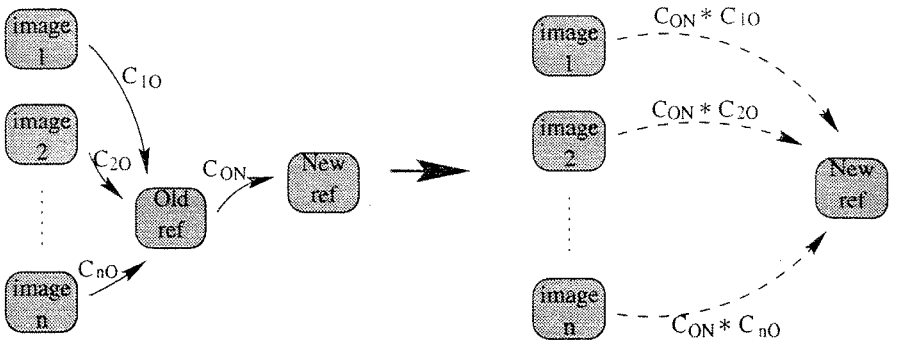

Fig. 6. Matrix combination to change the reference image.

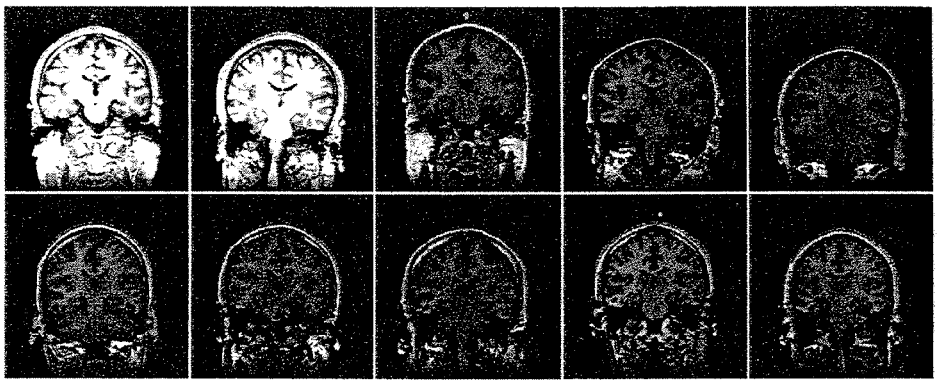

Fig. 7. Coronal slice of each image composing the database. Images are numbered from 1 to 10 when counting from left to right, top to bottom.

4.2. Data Sets

The following results were obtained using a database of 10 MR images of healthy subjects provided by Dr. Ron Kikinis of Brigham and Women's Hospital (see Fig. 7). Each image contains $256 \times 256 \times 123$ voxels each representing $1 \times 1 \times 1.5$ mm^3 with a possibility of 256 gray levels. A coronal slice of each of those images is shown in Fig. 7 in which the left side of the subject corresponds to the left side of the image. The images will be called $I_1, \ldots, I_{10}$, referring to the corresponding image when counting from left to right, top to bottom. All experiments were conducted on a DEC AlphaStation 400 4/233.

4.3. Results

We present the correction of morphometrical differences for a VOI in the left temporal lobe of the brain. The reference image is I_{10} in which we define a VOI of $64 \times 64 \times 20$ voxels of $1 \times 1 \times 1$ mm^3.

Figures 8–11 show the evolution of the VOIs throughout the correction procedure. The first image, Fig. 8, presents the VOIs taken before any processing. It exhibits the differences due to intensity and positioning. After the first step which consists of intensity corrections and elimination of global morphometrical differences, the VOIs seem much more similar (see Fig. 9).

Although affine dissimilarities are small, it is still possible to eliminate those variations by matching only the VOI images instead of the whole brain volume. Results of this second phase are shown in Fig. 10. They represent corresponding VOIs and their differences are due only to morphology and local morphometry.

The third step is to eliminate those local morphometrical differences. After this (see Fig. 11), we believe that only morphological differences are present.

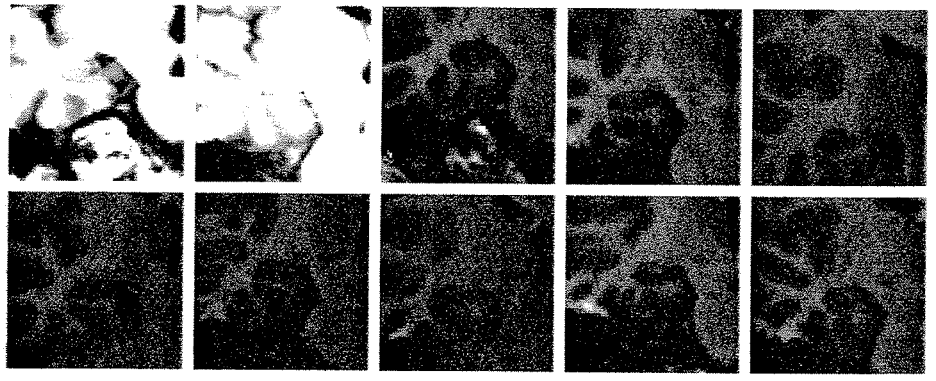

Fig. 8. VOIs without correction.

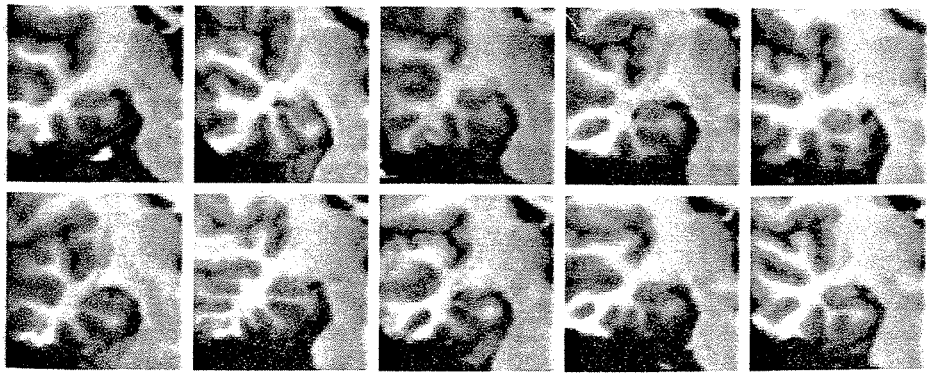

Fig. 9. VOIs after global correction.

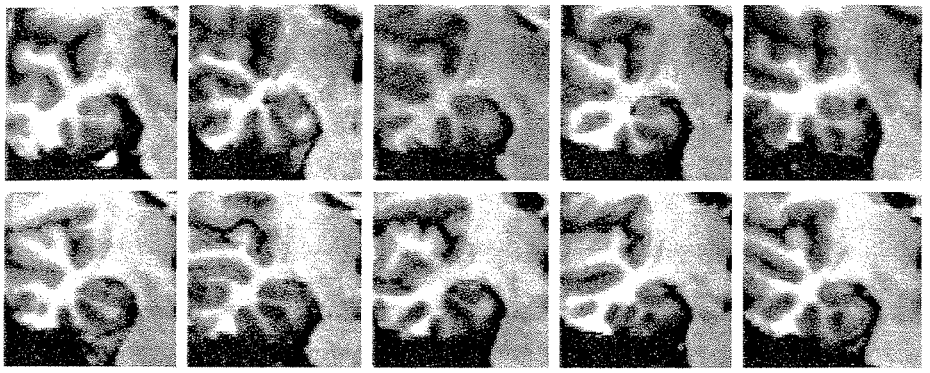

Fig. 10. VOIs after regional correction.

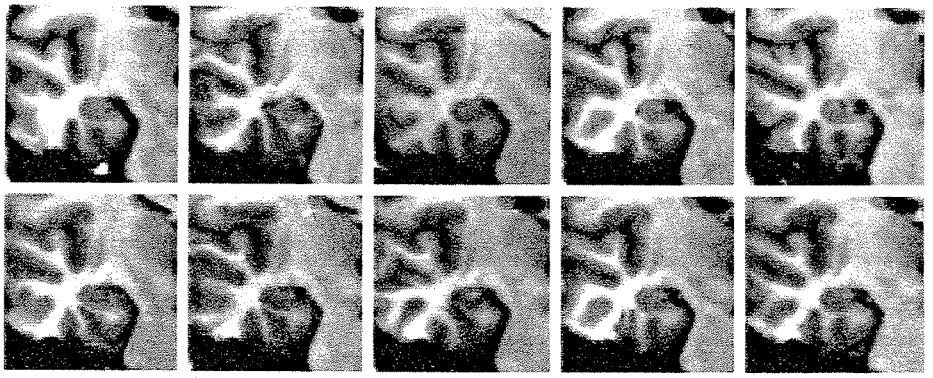

Fig. 11. VOIs after all morphometrical correction.

5. APPLICATIONS

Applications resulting from the correction of morphometrical differences could be divided in two categories: (1) studies of local morphometrical differences, or (2) studies of morphological variations.

5.1. Morphometrical Measures

This class of application relies on measures of brain structures, e.g. the comparisons of the basal ganglia's component volumes with a standard model to identify schizophrenia.[25] The construction of such a model relies on measures taken from a population of normal subjects. We have implemented this last idea.

5.1.1. Construction method

The idea behind the construction procedure is derived from Refs. 8, 16, 26 and 27 and consists of extracting from the database the volumes corresponding to a VOI

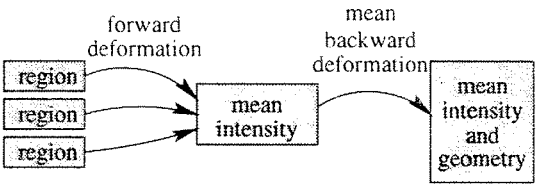

Fig. 12. Procedure to build an average VOI from a set of images.

defined on a reference image, and applying to the average of those VOIs the average of the local morphometrical differences. This process is depicted in Fig. 12.

Using the procedure described in Sec. 4.1 on all the entries of the database, we can eliminate global and regional morphometrical differences to extract corresponding VOIs of our database. For each of those entries, we can compute the displacement field that maps the entry VOI onto the reference VOI (forward) and the reference VOI onto the entry VOI (backward). These displacements account for local morphometrical differences. Applying to every region the forward displacement field produces images with the same morphometry as the reference VOI but with different intensities. Arithmetic averaging of corresponding voxel intensities between VOIs produces a mean intensity image with the morphometry of the reference image. Furthermore, by applying the average backward displacement field to this last image, we create a mean intensity and morphometry representation of our database, or the "average" VOI.

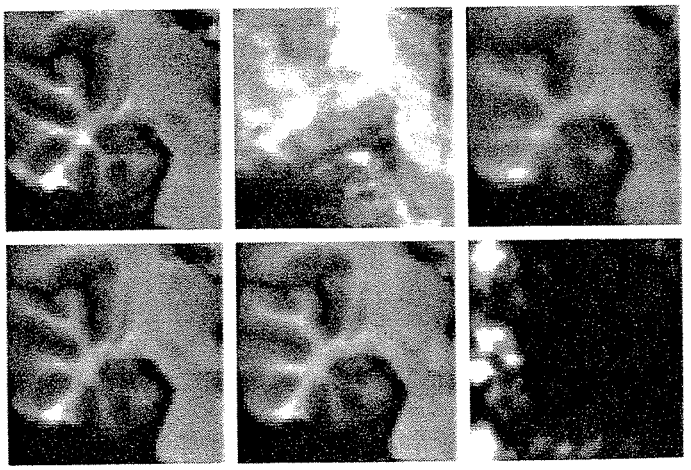

Fig. 13. Different types of "average" patients. **First line**: Original reference VOI; average of the 10 VOIs before any processing; average VOI after exclusion of global and regional morphometrical differences. **Second line**: average VOI without morphometrical differences (mean intensity); average backward deformation applied to the average VOI without morphometrical differences (mean intensity and morphometry); variance of the average backward deformation. See the text for explications.

5.1.2. Resulting "average" patients

Using all the computations up to now, we can obtain different kinds of "average" patients. Figure 13 shows such results. The first image is the reference VOI and is shown only for comparison purposes. To its right is a simple average of the VOIs taken from each subject previous to any warping, putting forward the different patient positions during the acquisition. The third image presents the average of corresponding volumes of the database. Structures which are morphologically stable appear well contrasted while unstable ones are fuzzy. The first image of the second line is the average of the VOI intensities after elimination of morphometrical differences. Deforming this image with the average backward displacement field creates an image that represents the mean intensity and morphometry of the database, or the average VOI. It has the remarkable property of being an average image while not suffering from severe smoothing. Finally, we present the variance of the backward deformation field amplitude obtained from our database as a simple display of the variability of the different structure positions.

An advantage of our technique is that the average images produced are of the quality similar to the MR images of the database. Hence the same inter-patient matching method can be applied to compare a new patient to the average, which is an alternative to whole database exploration.

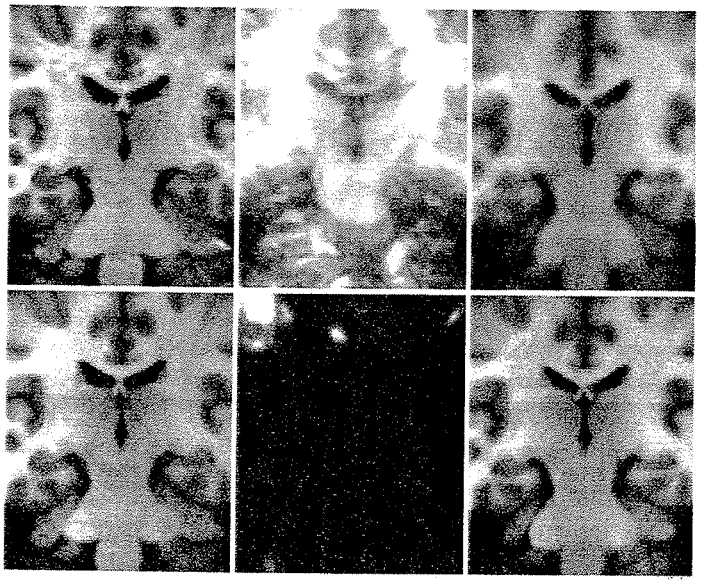

Fig. 14. Average VOI obtained from free-form registration (see Fig. 13 for explanations. The positions of the second and third images of the second line have been interchanged for comparison purposes.)

We have applied the same scheme to extract from the database the volumes that contain the ventricles. Averages have been built using the method previously explained and are shown in Fig. 14. The careful observer will notice that, although

they were obtained using different methods, the average VOI (last image of the second row) resembles a smoothed version of the average VOI after affine correction (last image of the first row). This is especially true for the ventricles and strengthens the theory behind our method.

In this case, we have also applied to the segmented ventricles, the displacement field corresponding to the average local morphometrical differences. This permitted the construction of ventricles that represent the average morphometry of our database. They are shown in Fig. 15: to the left, the original ventricles and to the right, a display of their average morphometry. An obvious difference is the back-end of the ventricles which are thinner for the average patient than for the original ventricles.

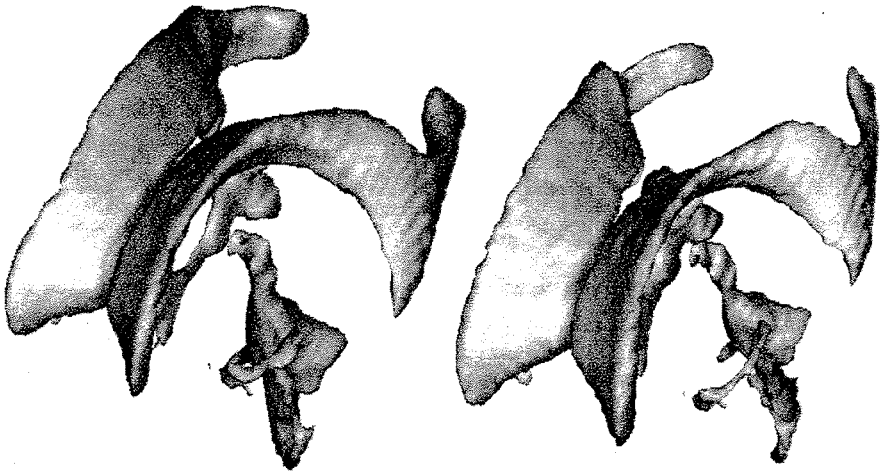

Fig. 15. Left: original ventricles. Right: morphometrical average ventricles of the database.

5.2. Morphological Measures

This class of applications is concerned with the presence or absence of features. Following this, we have just begun experiments to classify similar patients according to morphology. This work requires methods related to sorting subjects, or more generally, the development of similarity criteria. Despite the large literature on this topic,[28,29] our goal here is neither to find the best measure nor to analyze its relationship with our registration procedure. We wish to show practical applications of VOI extraction and evaluate qualitatively different similarity criteria. Hence, the following experiments are to be considered as first steps to a feasibility study. Furthermore, the images at our disposal are of normal subjects. Consequently, we are not trying to evaluate pathologies or find anomalies.

Among available choices, we have chosen two: (1) the stochastic sign-change (SSC), which is based on zero-crossings, and (2) correlation. The method consists of extracting morphometrically corresponding VOIs automatically from the

database using the method previously described. We then define a *working space* in which comparisons are done (see Fig. 16). We present the criteria used and show preliminary results of VOI classification according to their resemblance with I_{10}.

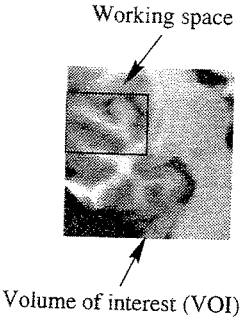

Fig. 16. A slice of the VOI and working space. Only the working space is considered for comparisons.

5.2.1. The stochastic sign-change criterion

This criterion was introduced by Venot *et al.*[30] for the comparison of scintigraphic images. It is a measure of similitude between two images and is based on zero-crossings (see Fig. 17).

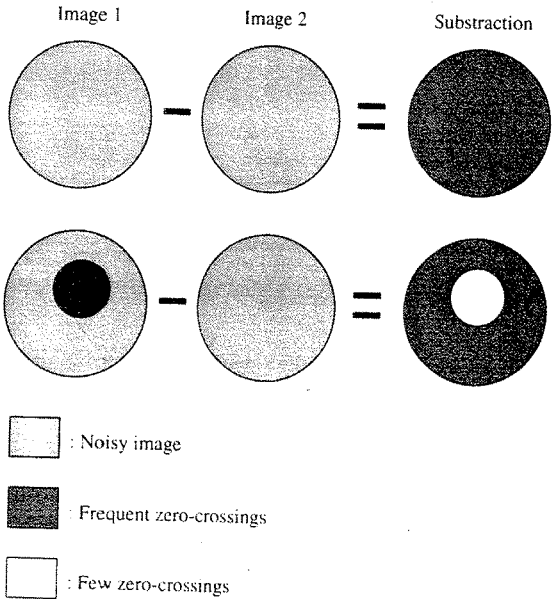

Fig. 17. The stochastic sign-change criterion.

Let I_1 and I_2 be similar images that contain noise and $S = I_1 - I_2$. Originally, I_1 and I_2 are identical. Then, S is not zero but contains sign fluctuations because of noise. However, if the two images differ from one another in some region R of S, R will contain either mostly positive or mostly negative values and the number of sign changes in S is reduced. This shows that a high SSC count in S is a good indication of the resemblance between two images.

To count the number of sign changes, we go through the subtraction image three times: once comparing values in the X direction, once in the Y direction and a last time for the Z direction. This criterion can be normalized by considering the maximal value of SSC in the working space. Hence, values close to 1 show good similitudes, and those close to 0, poor correspondence.

5.2.2. Correlation

The correlation between the two working spaces X and Y each containing N voxels is computed using the following formula:

$$\mathbf{Corr}(X,Y) = \frac{\mathbf{Cov}(X,Y)}{\sqrt{\mathbf{Var}(X)\mathbf{Var}(Y)}}$$

where

$$\mathbf{Cov}(X,Y) = \frac{1}{N}\sum_{i=1}^{N} X_i Y_i - \frac{1}{N^2}\sum_{i=1}^{N} X_i \sum_{i=1}^{N} Y_i$$
$$\mathbf{Var}(X) = \mathbf{Cov}(X,X)$$
$$\mathbf{Var}(Y) = \mathbf{Cov}(Y,Y)\,.$$

5.2.3. Results

The SSC values are sorted in Table 1 and the correlation coefficients in Table 2. We also present, using this ordering, the working spaces used for computations in Figs. 18 and 19. Each of these figures contains two non-adjacent slices of the

Table 1. Classification using the SSC criterion.

Image	SSC value (normalized)
10	1.000
4	0.325
7	0.315
6	0.305
9	0.285
5	0.284
3	0.282
2	0.279
8	0.271
1	0.268

Table 2. Classification using correlation.

Image	Correlation
10	1.000
4	0.917
6	0.906
3	0.906
1	0.888
7	0.879
5	0.858
9	0.845
8	0.844
2	0.836

First slice

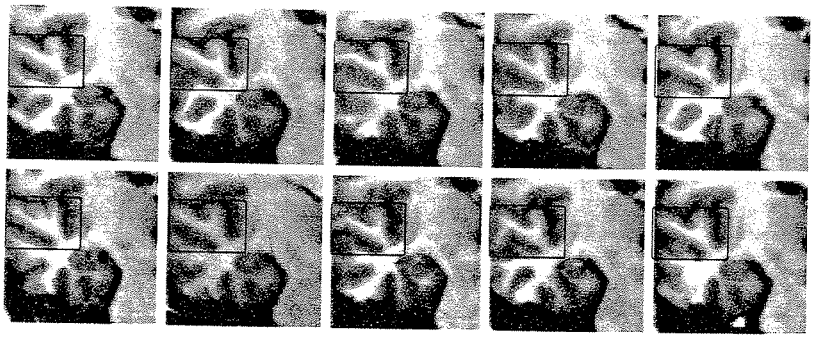

Second slice

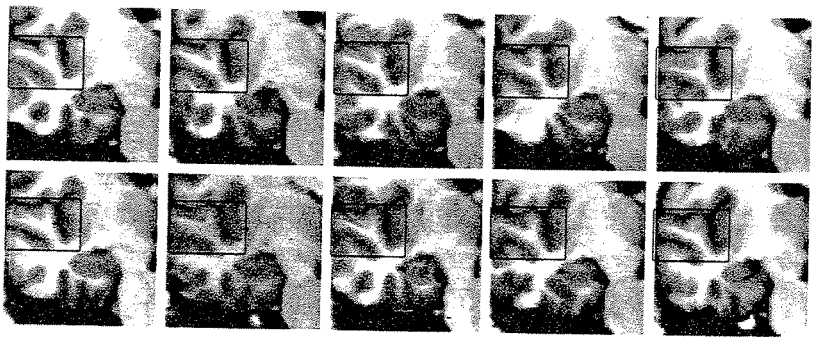

Fig. 18. Classification using the SSC criterion. Two volume slices are shown.

VOIs to get a better understanding of the tridimensional structure. They show the importance to our three-dimensional approach since one would probably change this disposition by only looking at one slice.

The ordering obtained with the SSC criterion and with the correlation are similar upto minor permutations. The only large difference has to do with I_1 which is

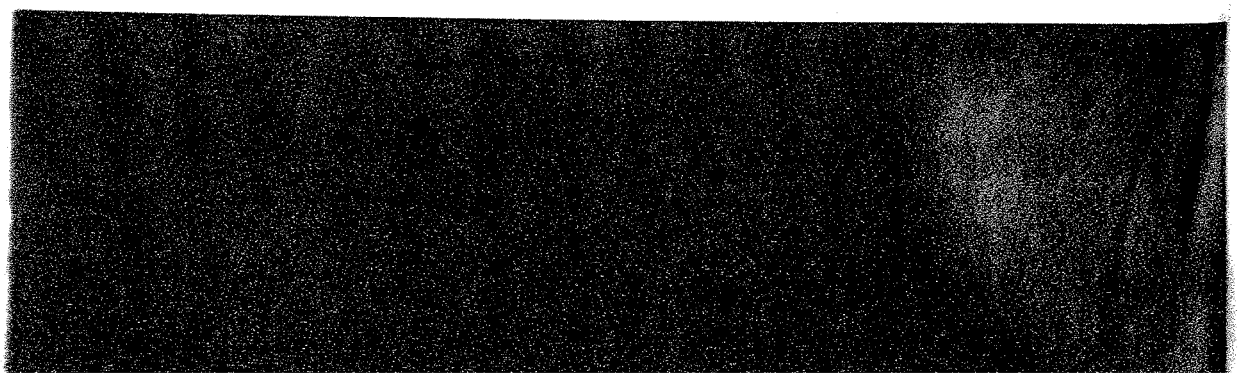

identified as having the most different morphology using the SSC criterion and is placed fifth using correlation. By looking at both slices of this VOI, we can see that it is quite similar to I_{10}. Hence, preliminary results seem to indicate that correlation would be more appropriate to evaluate morphological differences than the SSC criterion. On the light of those results, comparison bases on mutual information techniques are expected to give good classification.

Although in this case we used an elastic registration procedure before classification, when assuming negligible morphological variations, this classification method can be used on corresponding VOIs, thus using only affine transformation for registration purposes. In this case, an order on local morphometrical differences would be obtained.

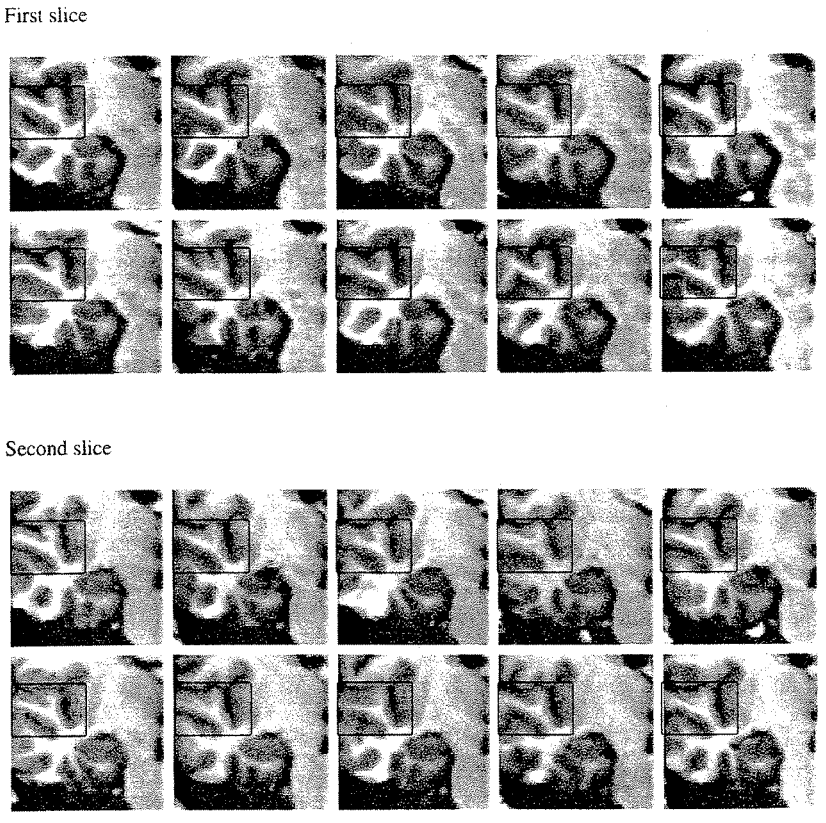

Fig. 19. Classification using correlation. Two volume slices are shown.

5.3. Discussion

The main benefit of this method is that it is fast and fairly robust. The time to obtain the corresponding VOIs varies between 5 and 10 seconds, and local warping doubles this time. This opens a new door on medical image database exploration.

It is now possible to retrieve a large amount of corresponding volumes in a reasonable amount of time. Once those volumes are extracted, further processing like classification and similarity matches can be operated to result in extrapolation of information contained in the database to other images. For example, this technology is presently being used for the study of morphometrical hippocampal variations in epileptic patients. We have only started to explore this field but preliminary results are encouraging.

6. CONCLUSION

We have presented a new method to obtain corresponding volumes of interest from medical image databases. This procedure has the advantage of restraining itself to local volumes of the brain and thus is not influenced by misleading information from other regions. It has been applied to the quantification of morphometrical and morphological variations. We believe that better results could be obtained by dividing subjects into subclasses of normal patients based on morphological similarities. This would facilitate the analysis of only morphometrical differences, to provide a better understanding of dissimilarities between a patient and the group of normal subjects with corresponding morphology.

Future applications and research on classification and extraction of similar patients for epidemiology statistics or computer aided diagnosis are envisioned. Such applications are a first step toward the extrapolation of information from an image database to other images.

ACKNOWLEDGMENTS

Thanks to Dr. Ron Kikinis of Brigham and Women's Hospital, Boston, for the MR images. Part of this work was funded by the Natural Sciences and Engineering and Research Council of Canada (NSERC), the Fonds pour la Formation de Chercheurs et l'Aide à la Recherche du Québec (FCAR), the Association des Directeurs de Recherche Industrielle du Québec (ADRIQ) and the Département d'Informatique et de Recherche Opérationnelle de l'Université de Montréal (DIRO).

REFERENCES

1. J. Talairach and P. Tournoux, *Co-Planar Stereotaxic Atlas of the Human Brain*, Thieme Medical Publishers, New York, United States, 1988.
2. G. Schaltenbrand and W. Wahren, *Atlas of Stereotaxy of the Human Brain*, Georg Thieme Verlag, Stuttgart, 1977.
3. E. Pernkopf, *Atlas d'Anatomie Humaine*, Piccin, 1983.
4. H. Braak, *Architectonics of the Human Telencephalic Cortex*, Springer-Verlag, Berlin, 1980.
5. J. C. Mazziotta, A. W. Toga, A. Evans, P. Fox and J. Landcaster, "A probabilistic atlas of the human brain: Theory and rationales for its development", *Neuroimage* **2** (1995) 89–101.
6. G. Subsol, *Construction Automatique d'Atlas Anatomiques Morphométriques à Partir d'Images Médicales Tridimensionnelles*, PhD thesis, École Centrale de Paris, 1995. Electronic version: http://www.inria.fr/RRRT/TU-0379.html.

7. A. W. Toga, P. Thompson and B. A. Payne, *Modeling Morphometric Changes of the Brain During Development*, Academic Press, 1996.
8. G. Subsol, J.-P. Thirion and N. Ayache, "Application of an automatically building 3D morphometric anatomical atlases: Applications to a skull atlas", *Medical Robotics and Computer Aided Surgery*, Baltimore (USA), Nov. 1995, pp. 226–233. Electronic version: http://www.inria.fr/RRRT/RR-2586.html.
9. A. Guéziec and N. Ayache, "Smoothing and matching of 3D space curves", *European Conf. Computer Vision*, Santa Margherita (Italy), Springer-Verlag, May 1992.
10. J. Feldmar and N. Ayache, "Rigid, affine and locally affine registration of free-form surfaces", *Int. J. Comput. Vision* **18**, 2 (1996) 99–119. Electronic version: http://www.inria.fr/RRRT/RR-2220.html.
11. R. Szeliski and S. Lavallée, "Matching 3-D anatomical surfaces with non-rigid deformations using octree-splines", *Int. J. Comput. Vision* **18**, 2 (1996) 171–186.
12. J.-P. Thirion, "Fast non-rigid matching 3D medical images", *Medical Robotics and Computer Aided Surgery*, Baltimore (USA), Nov. 1995, pp. 47–54. Electronic version: http://www.inria.fr/RRRT/RR-2547.html.
13. D. L. Collins, T. M. Peters and A. C. Evans, "An automated 3D nonlinear deformation procedure for determination of gross morphometric variability in human brain", in *Visualization in Biomedical Computing*, ed. R. A. Robb, vol. 2359 of *SPIE Proc.*, Rochester, Oct. 1994, pp. 180–190.
14. J. Gee, M. Reivich and R. Bajcsy, "Elastically deforming 3D atlas to match anatomical brain images", *J. Comput. Assist. Tomogr.* **17**, 2 (1993) 225–236.
15. M. Bro-Nielsen and C. Gramkow, "Fast fluid registration of medical images", in *Visualization in Biomedical Computing*, eds. K. H. Höhne and R. Kikinis, vol. 1131 of *Lecture Notes in Computer Science*, Hamburg (Germany), Springer, Sept. 1996.
16. D. L. Collins, P. Neelin, T. M. Peters and A. C. Evans, "Automatic 3D intersubject registration of MR volumetric data in standardized Talairach space", *J. Comput. Assist. Tomogr.* **18**, 2 (1992) 205.
17. N. C. Andreasen, S. Arndt, V. Swayze II, T. Cizadlo, M. Flaum, D. O'Leary, J. C. Ehrhardt and W. T. Yuh, "Thalamic abnormalies in schizophrenia visualized through magnetic resonance image averaging", *Science* **266** (1994) 294–298.
18. J. Martin, A. Pentland, S. Sclaroff and R. Kikinis, "Characterization of neuropathological shape deformations", Technical Report 331, M.I.T. Media Laboratory Perceptual Computing, May 1995.
19. D. Lemoine, C. Barillot, B. Gibaud and E. Pasqualini, "An anatomical-based 3D registration of multi-modality and atlas data in surgery", in *Information Processing in Medical Imaging*, eds. A. Colchester and D. Hawkes, Springer-Verlag, Wye (UK), 1991, p. 188.
20. T. Greitz, C. Bohm, S. Holte and L. Eriksson, "A computerized brain atlas: Construction, anatomical content, and some applications", *J. Comput. Assist. Tomogr.* **15**, 1 (1991) 26–38.
21. J. Declerck, G. Subsol, J.-P. Thirion and N. Ayache, "Automatic retrieval of anatomical structures in 3D medical images", in *Conf. Computer Vision, Virtual Reality and Robotics in Medicine*, ed. N. Ayache, vol. 905 of *Lecture Notes in Computer Science*, Springer-Verlag, Nice (France), Apr. 1995, pp. 153–162. Electronic version: http://www.inria.fr/RRRT/RR-2485.html.
22. R. Bajcsy and S. Kovačič, "Multiresolution elastic matching", *Comput. Vision Graphics Imag. Process.* **46** (1989) 1–21.
23. G. E. Christensen, M. I. Miller and M. Vannier, "A 3D brain mapping using a deformable neuroanatomy", *Phys. Med. Biol.* **39** (1994) 609–618.

24. J.-P. Thirion, "Non-rigid matching using demons", *Computer Vision and Pattern Recognition*, San Francisco (USA), June 1996. Electronic version: http://www.inria.fr/RRRT/RR-2547.html.
25. H. Hokama, M. E. Shenton, P. G. Nestor, R. Kikinis, J. J. Levitt, D. Metcalf, C. G. Wible, B. F. O'Donnell, F. A. Jolesz and R. W. McCarley, "Caudate, putamen, and globus pallidus volume in schizophrenia: A quantitative MRI study", *Psychiatry Research: Neuroimaging* **61** (1995) 209–229.
26. G. Subsol, J.-P. Thirion and N. Ayache, "A general scheme for automatically building 3D morphometric anatomical atlases: Applications to a skull atlas", *Medical Robotics and Computer Aided Surgery*, Baltimore (USA), Nov. 1995, pp. 373–382. Electronic version: http://www.iniria.fr/RRRT/RR-2586.html.
27. J.-P. Thirion, G. Subsol and D. Dean, "Cross validation of three inter-patients matching methods", in *Visualization in Biomedical Computing*, vol. 1131 of *Lecture Notes in Computer Science*, eds. K. H. Höhne and R. Kikinis, Springer-Verlag, Hamburg (Germany), Sept. 1996, pp. 327–336.
28. K. Fukunaga, *Introduction to Statistical Pattern Recognition*, Computer Science and Scientific Computing, Academic Press, 2nd ed., 1990.
29. T. Pavlidis, *Structural Pattern Recognition*, vol. 1 of *Springer Series in Electrophysics*, Springer-Verlag, New York, 1977.
30. A. Venot, J. Lebruchec, J. Golmard and J. Roucavrol, "An automated method for the normalization of scintigraphic images", *J. Nuclear Med.* **24** (1983) 529–531.

Alexandre Guimond received his B.Sc. in computer science from the Université de Montréal in 1995. He is currently pursuing a Ph.D. degree in computer science at both the Université de Montréal and the Université de Nice within the EPIDAURE Project of INRIA.

His research interest is directed towards the analysis of anatomical variations within the human brain using magnetic resonance imaging.

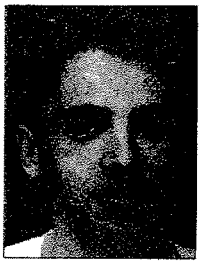

Gérard Subsol is a research engineer with the EPIDAURE Project of INRIA. He obtained his Ph.D. in computer science from the École Centrale de Paris, with high honours in 1995.

His research deals with the development of a method (inter-patient registration, quantitative analysis of the shape) to build automatically morphometrical atlases from 3D medical images (e.g. brain or skull). He is currently involved in the European Project BIOMORPH that aims to develop new tools to analyze the brain morphology.

J.-P. Thirion graduated from the École Normale Sup'erieure de Paris in 1984. He received his Ph.D. in computer science from the Université Paris XI (Orsay) in 1990 for his research in the E.N.S. project iMAGIS.

From 1990 to 1997, he worked as a research scientist in the EPIDAURE project at INRIA Sophia Antipolis in medical image analysis. His primary work regards rigid and non-rigid registration algorithms. He currently occupies the Research and Development Vice-President's position at Focus Imaging and is on the editorial board of MEDIA (Medical Image Analysis).

ISSN: 0218-0014

INTERNATIONAL JOURNAL OF PATTERN RECOGNITION AND ARTIFICIAL INTELLIGENCE

Vol. [illegible] • Number 3 • Decembe[illegible]

Special issue

PROCESSING OF MR IMAGES OF THE HUMAN BRAIN

Edited by **H. Pien, W. C. Karl, D. Kennedy**
A. Worth and **A. Willsky**

World Scientific